

Measurements of the branching fractions of semileptonic decays $\Xi_c^0 \rightarrow \Xi^- \ell^+ \nu_\ell$ and asymmetry parameter of $\Xi_c^0 \rightarrow \Xi^- \pi^+$ decay

Y. B. Li,¹² C. P. Shen,¹² I. Adachi,^{19, 15} K. Adamczyk,⁶⁰ H. Aihara,⁸³ S. Al Said,^{76, 37} D. M. Asner,³ T. Aushev,²⁰ R. Ayad,⁷⁶ V. Babu,⁸ P. Behera,²⁶ J. Bennett,⁵² M. Bessner,¹⁸ V. Bhardwaj,²³ B. Bhuyan,²⁴ T. Bilka,⁵ J. Biswal,³⁴ G. Bonvicini,⁸⁶ A. Bozek,⁶⁰ T. E. Browder,¹⁸ M. Campajola,^{31, 55} D. Červenkov,⁵ M.-C. Chang,¹¹ A. Chen,⁵⁷ B. G. Cheon,¹⁷ K. Chilikin,⁴⁴ K. Cho,³⁹ S.-J. Cho,⁸⁸ S.-K. Choi,¹⁶ Y. Choi,⁷⁴ S. Choudhury,²⁵ D. Cinabro,⁸⁶ S. Cunliffe,⁸ S. Das,⁴⁹ N. Dash,²⁶ G. De Nardo,^{31, 55} R. Dhamija,²⁵ F. Di Capua,^{31, 55} T. V. Dong,¹² S. Eidelman,^{4, 63, 44} D. Epifanov,^{4, 63} T. Ferber,⁸ B. G. Fulsom,⁶⁵ R. Garg,⁶⁶ V. Gaur,⁸⁵ N. Gabyshev,^{4, 63} A. Garmash,^{4, 63} A. Giri,²⁵ P. Goldenzweig,³⁵ O. Grzymkowska,⁶⁰ K. Gudkova,^{4, 63} C. Hadjivasiliou,⁶⁵ O. Hartbrich,¹⁸ K. Hayasaka,⁶² H. Hayashii,⁵⁶ M. Hernandez Villanueva,⁵² C.-L. Hsu,⁷⁵ A. Ishikawa,^{19, 15} R. Itoh,^{19, 15} M. Iwasaki,⁶⁴ Y. Iwasaki,¹⁹ W. W. Jacobs,²⁷ S. Jia,¹² Y. Jin,⁸³ C. W. Joo,³⁶ K. K. Joo,⁶ K. H. Kang,⁴² G. Karyan,⁸ Y. Kato,⁵⁴ H. Kichimi,¹⁹ C. H. Kim,¹⁷ D. Y. Kim,⁷³ K.-H. Kim,⁸⁸ S. H. Kim,⁷¹ K. Kinoshita,⁷ P. Kodyš,⁵ T. Konno,³⁸ A. Korobov,^{4, 63} S. Korpar,^{50, 34} E. Kovalenko,^{4, 63} P. Križan,^{46, 34} R. Kroeger,⁵² P. Krokovny,^{4, 63} T. Kuhr,⁴⁷ M. Kumar,⁴⁹ R. Kumar,⁶⁸ K. Kumara,⁸⁶ A. Kuzmin,^{4, 63} Y.-J. Kwon,⁸⁸ K. Lalwani,⁴⁹ J. S. Lange,¹³ I. S. Lee,¹⁷ S. C. Lee,⁴² C. H. Li,⁴⁵ L. K. Li,⁷ L. Li Gioi,⁵¹ J. Libby,²⁶ K. Lieret,⁴⁷ D. Liventsev,^{86, 19} M. Masuda,^{82, 69} D. Matvienko,^{4, 63, 44} J. T. McNeil,¹⁰ F. Metzner,³⁵ R. Mizuk,^{44, 20} G. B. Mohanty,⁷⁷ T. J. Moon,⁷¹ T. Mori,⁵⁴ R. Mussa,³² A. Natochii,¹⁸ L. Nayak,²⁵ M. Nayak,⁷⁹ M. Niiyama,⁴¹ N. K. Nisar,³ S. Nishida,^{19, 15} K. Nishimura,¹⁸ S. Ogawa,⁸⁰ H. Ono,^{61, 62} Y. Onuki,⁸³ P. Pakhlov,^{44, 53} G. Pakhlova,^{20, 44} T. Pang,⁶⁷ S. Pardi,³¹ H. Park,⁴² S. Patra,²³ S. Paul,^{78, 51} T. K. Pedlar,⁴⁸ R. Pestotnik,³⁴ L. E. Piilonen,⁸⁵ T. Podobnik,^{46, 34} V. Popov,²⁰ E. Prencipe,²¹ M. T. Prim,² M. Röhrken,⁸ A. Rostomyan,⁸ N. Rout,²⁶ G. Russo,⁵⁵ D. Sahoo,⁷⁷ Y. Sakai,^{19, 15} S. Sandilya,²⁵ L. Santelj,^{46, 34} T. Sanuki,⁸¹ V. Savinov,⁶⁷ G. Schnell,^{1, 22} C. Schwanda,²⁹ Y. Seino,⁶² K. Senyo,⁸⁷ M. Shapkin,³⁰ C. Sharma,⁴⁹ J.-G. Shiu,⁵⁹ A. Sokolov,³⁰ E. Solovieva,⁴⁴ M. Starič,³⁴ Z. S. Stottler,⁸⁵ M. Sumihama,¹⁴ U. Tamponi,³² K. Tanida,³³ F. Tenchini,⁸ M. Uchida,⁸⁴ S. Uehara,^{19, 15} T. Uglov,^{44, 20} K. Uno,⁶² S. Uno,^{19, 15} Y. Usov,^{4, 63} R. Van Tonder,² G. Varner,¹⁸ A. Vinokurova,^{4, 63} A. Vossen,⁹ C. H. Wang,⁵⁸ M.-Z. Wang,⁵⁹ P. Wang,²⁸ X. L. Wang,¹² M. Watanabe,⁶² S. Watanuki,⁴³ E. Won,⁴⁰ X. Xu,⁷² W. Yan,⁷⁰ S. B. Yang,⁴⁰ H. Ye,⁸ J. H. Yin,⁴⁰ C. Z. Yuan,²⁸ Z. P. Zhang,⁷⁰ V. Zhilich,^{4, 63} and V. Zhukova⁴⁴

(The Belle Collaboration)

¹Department of Physics, University of the Basque Country UPV/EHU, 48080 Bilbao

²University of Bonn, 53115 Bonn

³Brookhaven National Laboratory, Upton, New York 11973

⁴Budker Institute of Nuclear Physics SB RAS, Novosibirsk 630090

⁵Faculty of Mathematics and Physics, Charles University, 121 16 Prague

⁶Chonnam National University, Gwangju 61186

⁷University of Cincinnati, Cincinnati, Ohio 45221

⁸Deutsches Elektronen-Synchrotron, 22607 Hamburg

⁹Duke University, Durham, North Carolina 27708

¹⁰University of Florida, Gainesville, Florida 32611

¹¹Department of Physics, Fu Jen Catholic University, Taipei 24205

¹²Key Laboratory of Nuclear Physics and Ion-beam Application (MOE)

and Institute of Modern Physics, Fudan University, Shanghai 200443

¹³Justus-Liebig-Universität Gießen, 35392 Gießen

¹⁴Gifu University, Gifu 501-1193

¹⁵SOKENDAI (The Graduate University for Advanced Studies), Hayama 240-0193

¹⁶Gyeongsang National University, Jinju 52828

¹⁷Department of Physics and Institute of Natural Sciences, Hanyang University, Seoul 04763

¹⁸University of Hawaii, Honolulu, Hawaii 96822

¹⁹High Energy Accelerator Research Organization (KEK), Tsukuba 305-0801

²⁰Higher School of Economics (HSE), Moscow 101000

²¹Forschungszentrum Jülich, 52425 Jülich

²²IKERBASQUE, Basque Foundation for Science, 48013 Bilbao

²³Indian Institute of Science Education and Research Mohali, SAS Nagar, 140306

²⁴Indian Institute of Technology Guwahati, Assam 781039

²⁵Indian Institute of Technology Hyderabad, Telangana 502285

²⁶Indian Institute of Technology Madras, Chennai 600036

²⁷Indiana University, Bloomington, Indiana 47408
²⁸Institute of High Energy Physics, Chinese Academy of Sciences, Beijing 100049
²⁹Institute of High Energy Physics, Vienna 1050
³⁰Institute for High Energy Physics, Protvino 142281
³¹INFN - Sezione di Napoli, 80126 Napoli
³²INFN - Sezione di Torino, 10125 Torino
³³Advanced Science Research Center, Japan Atomic Energy Agency, Naka 319-1195
³⁴J. Stefan Institute, 1000 Ljubljana
³⁵Institut für Experimentelle Teilchenphysik, Karlsruher Institut für Technologie, 76131 Karlsruhe
³⁶Kavli Institute for the Physics and Mathematics of the Universe (WPI), University of Tokyo, Kashiwa 277-8583
³⁷Department of Physics, Faculty of Science, King Abdulaziz University, Jeddah 21589
³⁸Kitasato University, Sagamihara 252-0373
³⁹Korea Institute of Science and Technology Information, Daejeon 34141
⁴⁰Korea University, Seoul 02841
⁴¹Kyoto Sangyo University, Kyoto 603-8555
⁴²Kyungpook National University, Daegu 41566
⁴³Université Paris-Saclay, CNRS/IN2P3, IJCLab, 91405 Orsay
⁴⁴P.N. Lebedev Physical Institute of the Russian Academy of Sciences, Moscow 119991
⁴⁵Liaoning Normal University, Dalian 116029
⁴⁶Faculty of Mathematics and Physics, University of Ljubljana, 1000 Ljubljana
⁴⁷Ludwig Maximilians University, 80539 Munich
⁴⁸Luther College, Decorah, Iowa 52101
⁴⁹Malaviya National Institute of Technology Jaipur, Jaipur 302017
⁵⁰University of Maribor, 2000 Maribor
⁵¹Max-Planck-Institut für Physik, 80805 München
⁵²University of Mississippi, University, Mississippi 38677
⁵³Moscow Physical Engineering Institute, Moscow 115409
⁵⁴Graduate School of Science, Nagoya University, Nagoya 464-8602
⁵⁵Università di Napoli Federico II, 80126 Napoli
⁵⁶Nara Women's University, Nara 630-8506
⁵⁷National Central University, Chung-li 32054
⁵⁸National United University, Miao Li 36003
⁵⁹Department of Physics, National Taiwan University, Taipei 10617
⁶⁰H. Niewodniczanski Institute of Nuclear Physics, Krakow 31-342
⁶¹Nippon Dental University, Niigata 951-8580
⁶²Niigata University, Niigata 950-2181
⁶³Novosibirsk State University, Novosibirsk 630090
⁶⁴Osaka City University, Osaka 558-8585
⁶⁵Pacific Northwest National Laboratory, Richland, Washington 99352
⁶⁶Panjab University, Chandigarh 160014
⁶⁷University of Pittsburgh, Pittsburgh, Pennsylvania 15260
⁶⁸Punjab Agricultural University, Ludhiana 141004
⁶⁹Research Center for Nuclear Physics, Osaka University, Osaka 567-0047
⁷⁰Department of Modern Physics and State Key Laboratory of Particle Detection and Electronics, University of Science and Technology of China, Hefei 230026
⁷¹Seoul National University, Seoul 08826
⁷²Soochow University, Suzhou 215006
⁷³Soongsil University, Seoul 06978
⁷⁴Sungkyunkwan University, Suwon 16419
⁷⁵School of Physics, University of Sydney, New South Wales 2006
⁷⁶Department of Physics, Faculty of Science, University of Tabuk, Tabuk 71451
⁷⁷Tata Institute of Fundamental Research, Mumbai 400005
⁷⁸Department of Physics, Technische Universität München, 85748 Garching
⁷⁹School of Physics and Astronomy, Tel Aviv University, Tel Aviv 69978
⁸⁰Toho University, Funabashi 274-8510
⁸¹Department of Physics, Tohoku University, Sendai 980-8578
⁸²Earthquake Research Institute, University of Tokyo, Tokyo 113-0032
⁸³Department of Physics, University of Tokyo, Tokyo 113-0033
⁸⁴Tokyo Institute of Technology, Tokyo 152-8550
⁸⁵Virginia Polytechnic Institute and State University, Blacksburg, Virginia 24061
⁸⁶Wayne State University, Detroit, Michigan 48202
⁸⁷Yamagata University, Yamagata 990-8560
⁸⁸Yonsei University, Seoul 03722

Using a data sample of 89.5 fb^{-1} recorded at the energy $\sqrt{s} = 10.52 \text{ GeV}$ with the Belle detector at the KEKB e^+e^- collider, we report measurements of branching fractions of semileptonic decays $\Xi_c^0 \rightarrow \Xi^-\ell^+\nu_\ell$ ($\ell = e$ or μ). Furthermore, based on an additional data sample of 711 fb^{-1} at $\sqrt{s} = 10.58 \text{ GeV}$, the CP -asymmetry parameter of $\Xi_c^0 \rightarrow \Xi^-\pi^+$ decay is extracted. The branching fractions are measured to be $\mathcal{B}(\Xi_c^0 \rightarrow \Xi^-e^+\nu_e) = (1.72 \pm 0.10 \pm 0.12 \pm 0.50)\%$ and $\mathcal{B}(\Xi_c^0 \rightarrow \Xi^-\mu^+\nu_\mu) = (1.71 \pm 0.17 \pm 0.13 \pm 0.50)\%$ with much improved precision compared to the current world average. The first and the second uncertainty are statistical and systematic, respectively, while the third one arises due to the uncertainty of the $\Xi_c^0 \rightarrow \Xi^-\pi^+$ branching fraction. The corresponding ratio $\mathcal{B}(\Xi_c^0 \rightarrow \Xi^-e^+\nu_e)/\mathcal{B}(\Xi_c^0 \rightarrow \Xi^-\mu^+\nu_\mu)$ is $1.00 \pm 0.11 \pm 0.09$, which is consistent with the expectation of lepton flavor universality. The first measured asymmetry parameter is found to be consistent with zero, $\mathcal{A}_{CP} = (\alpha_{\Xi^-\pi^+} + \alpha_{\Xi^+\pi^-})/(\alpha_{\Xi^-\pi^+} - \alpha_{\Xi^+\pi^-}) = 0.015 \pm 0.052 \pm 0.017$.

Charmed baryons play an important role in studies of strong and weak interactions, especially via investigations of their semileptonic decays [1–3] and charge-parity violation (CPV) [4, 5]. Such decay amplitudes are the product of a well-understood leptonic current for the lepton system and a more complicated hadronic current for the quark transition. For semileptonic decays of SU(3) anti-triplets, Λ_c^+ and $\Xi_c^{+,0}$, thanks to the spin-zero light diquark constituents, a simpler and more powerful theoretical calculation of form factors, hadronic structures, and nonperturbative aspects of strong interactions can be performed in a relatively simple version of quantum chromodynamics (QCD) [1].

Thus far only semileptonic decays of Λ_c^+ have been comprehensively studied and are statistically limited by low production rates and/or high background levels of current experiments. Within uncertainties CP symmetry and lepton flavor universality (LFU) are found to be conserved [6–9]. A violation of LFU would be a clear sign of new physics [10–14]. The tantalizing deviation from Standard Model predictions in $b \rightarrow c\ell\nu$ and $b \rightarrow s\ell\ell$ processes [15–17] inspires tests of LFU in more semileptonic decays of heavy quarks. For Ξ_c^0 , the ARGUS collaboration first observed $18.1 \pm 5.9 \text{ }\Xi_c^0 \rightarrow \Xi\ell X$ events ($\ell = e$ or μ) [18]. Later, the CLEO collaboration found $54 \pm 10 \text{ }\Xi_c^0 \rightarrow \Xi^-e^+\nu_e$ events [19]. The ratio of the branching fractions, $\mathcal{B}(\Xi_c^0 \rightarrow \Xi^-e^+\nu_e)/\mathcal{B}(\Xi_c^0 \rightarrow \Xi^-\pi^+)$, was $0.96 \pm 0.43 \pm 0.18$ from ARGUS and $3.1 \pm 1.0 \pm 0.3$ from CLEO measurements, respectively. With the absolute branching fraction $\mathcal{B}(\Xi_c^0 \rightarrow \Xi^-\pi^+) = (1.80 \pm 0.52)\%$ measured by Belle recently [20], the averaged $\mathcal{B}(\Xi_c^0 \rightarrow \Xi^-e^+\nu_e)$ is $(2.34 \pm 1.59)\%$ [21]. A variety of models have been developed to predict the decay branching fraction for $\mathcal{B}(\Xi_c^0 \rightarrow \Xi^-e^+\nu_e)$ resulting in a range from 1.35% to $(7.28 \pm 2.54)\%$ [22–26]. A precise measurement is crucial to test these models as well as to constrain the model parameters.

Though the Standard Model accommodates CPV which is one of the conditions needed to explain our matter-dominated universe [27], the magnitude of this effect as predicted by the KM mechanism is not sufficient [28]. CPV has been established in many meson decays [29–37], but for baryons, only a 3.3σ evidence for

CPV in $\Lambda_b^0 \rightarrow p\pi^-\pi^+\pi^+$ has been found [38]. Studies of CP -violating processes in charm baryon sector are very scarce [8, 9]. Since there should be CPV sources other than currently known, it is imperative to search for those also in the charm baryon sector. Several models predict both the decay rates and the degree of parity violation in charmed baryon decays [39–46].

For the $\Xi_c^0 \rightarrow \Xi^-\pi^+ \rightarrow \Lambda\pi^-\pi^+$ process, the decay parameter $\alpha_{\Xi^-\pi^+}$ (denoted as α^+) enters the angular distribution expression,

$$\frac{dN}{d\cos\theta_\Xi} \propto 1 + \alpha_{\Xi^-\pi^+}\alpha_{\Xi^-}\cos\theta_\Xi. \quad (1)$$

Here, θ_Ξ is the angle between the Λ momentum vector and the opposite of the Ξ_c^0 momentum in the Ξ^- rest frame [47], dN is the number of signal events in each $\cos\theta_\Xi$ bin, and α_{Ξ^-} is decay parameter of Ξ^- [21]. The definition of $\alpha_{\Xi^+\pi^-}$ (denoted as α^-) is analogous to the charge-conjugated decay mode. The only charge-averaged measurement of the decay parameters $\alpha_{\Xi\pi}$ is from CLEO with the result $-0.56 \pm 0.39^{+0.10}_{-0.09}$ [48], which falls in the range of $[-0.99, -0.38]$ from theoretical predictions [42, 44, 45, 49–51]. The CP asymmetry parameter $\mathcal{A}_{CP} = (\alpha^+ + \alpha^-)/(\alpha^+ - \alpha^-)$ can be calculated for $\Xi_c^0 \rightarrow \Xi^-\pi^+$ and $\bar{\Xi}_c^0 \rightarrow \bar{\Xi}^+\pi^-$.

In this Letter, we present the measurements of the branching fractions for $\Xi_c^0 \rightarrow \Xi^-\ell^+\nu_\ell$ [52] with significantly improved precision using a data sample of 89.5 fb^{-1} collected at $\sqrt{s} = 10.52 \text{ GeV}$ by the Belle detector [53] at the KEKB asymmetric-energy collider [54]. Charm baryons are produced in processes such as $e^+e^- \rightarrow c\bar{c} \rightarrow \Xi_c^0 + \text{anything}$. Ξ^- is reconstructed via the $\Lambda\pi^-$ mode, and Λ decays into $p\pi^-$. LFU is checked using measured results. Using an additional data sample of 711 fb^{-1} at $\sqrt{s} = 10.58 \text{ GeV}$, decay parameters of α^+ and α^- and the CP -asymmetry parameter \mathcal{A}_{CP} are first measured for $\Xi_c^0 \rightarrow \Xi^-\pi^+$. The data sample at $\sqrt{s} = 10.58 \text{ GeV}$ is not used in the semileptonic decay analysis due to the complicated backgrounds from B decays which can not be described by a data-driven method.

To optimize the signal selection criteria and calculate the signal reconstruction efficiency, we use Monte Carlo (MC) simulated events. The $e^+e^- \rightarrow c\bar{c}$ process is simulated with PYTHIA [55], while the signal events of Ξ_c^0

semileptonic decays are generated using the form factor from Lattice QCD calculation [56], and $\Xi_c^0 \rightarrow \Xi^- \pi^+$ decays are generated with EVTGEN [57]. The MC events are processed with a detector simulation based on GEANT3 [58]. Generic MC samples of $\Upsilon(4S) \rightarrow B\bar{B}$ events with $B = B^+$ or B^0 , and $e^+e^- \rightarrow q\bar{q}$ events with $q = u, d, s, c$ at $\sqrt{s} = 10.52$ GeV and 10.58 GeV are used as background samples.

Except for the charged tracks from $\Lambda \rightarrow p\pi^-$ decay, the impact parameters perpendicular to and along the e^+ beam direction with respect to the interaction point are required to be less than 0.5 cm and 4 cm, respectively, and transverse momentum is restricted to be higher than 0.1 GeV/c. For charged tracks, information from different detector subsystems is combined to form the likelihood \mathcal{L}_i for species (i), where $i = e, \mu, \pi, K$, or p [59]. A track not from Λ with a likelihood ratio $\mathcal{L}_\pi/(\mathcal{L}_K + \mathcal{L}_\pi) > 0.6$ is identified as a pion. With this selection, the pion identification efficiency is about 94%, while 5% of the kaons are misidentified as pions. A track with a likelihood ratio $\mathcal{L}_e/(\mathcal{L}_e + \mathcal{L}_{\text{non-}e}) > 0.9$ is identified as an electron [60]. The γ conversions are removed by examining all combinations of an e^- candidate with other positrons in the event, and requiring e^+e^- invariant mass larger than 0.2 GeV/c². Tracks with $\mathcal{L}_\mu/(\mathcal{L}_\mu + \mathcal{L}_K + \mathcal{L}_\pi) > 0.9$ are considered as muon candidates [61]. Furthermore, the muon tracks are required to hit at least five layers of the K_L^0 and muon subdetector, and not to be identified as kaons with $\mathcal{L}_K/(\mathcal{L}_K + \mathcal{L}_\pi) < 0.4$ to suppress backgrounds due to misidentification. With the above selections, the efficiencies of electron and muon identifications are 96% and 75%, respectively, with the pion fake rates less than 2%.

Candidate Λ baryons are reconstructed in the decay $\Lambda \rightarrow p\pi^-$ and selected if $|M_{p\pi^-} - m_\Lambda| < 3$ MeV/c² ($\sim 2.5 \sigma$), where σ denotes the mass resolution. Here and throughout the text, M_i represents a measured invariant mass and m_i denotes the nominal mass of the particle i [21]. The proton track from Λ decay is required to satisfy $\mathcal{L}_p/(\mathcal{L}_\pi + \mathcal{L}_p) > 0.2$ and $\mathcal{L}_p/(\mathcal{L}_K + \mathcal{L}_p) > 0.2$ with an efficiency of 95%. We define the Ξ^- signal region as $|M_{\Lambda\pi^-} - m_{\Xi^-}| < 6.5$ MeV/c² ($\sim 3\sigma$), and Ξ^- mass sidebands as $1.294 \text{ GeV}/c^2 < M_{\Lambda\pi^-} < 1.307 \text{ GeV}/c^2$ and $1.337 \text{ GeV}/c^2 < M_{\Lambda\pi^-} < 1.350 \text{ GeV}/c^2$. To suppress the combinational background, we require the flight directions of Λ and Ξ^- candidates, which are reconstructed from their fitted production and decay vertices, to be within five degrees of their momentum directions. We also require the scaled momentum $p_{\Xi^-X}^*/p_{\text{max}}^* > 0.45$ ($X = e^+, \mu^+$ or π^+), where $p_{\Xi^-X}^*$ is the momentum of Ξ^-X system in the center-of-mass frame and $p_{\text{max}}^* \equiv \sqrt{E_{\text{beam}}^2 - m_{\Xi_c^0}^2}$ (E_{beam} is the beam energy). This requirement removes all $\Xi_c^0 \rightarrow \Xi^- \pi^+$ decays with Ξ_c^0 produced in B decays from

the $\sqrt{s} = 10.58$ GeV sample. For $\Xi_c^0 \rightarrow \Xi^- \ell^+ \nu_\ell$, the cosine of the opening angle between Ξ^- and ℓ^+ is further required to be larger than 0.25.

After the above selections, the obtained $\Xi^- e^+$, $\Xi^- \mu^+$, and $\Xi_c^0 \rightarrow \Xi^- \pi^+$ mass spectra in $p_{\Xi^-X}^*/p_{\text{max}}^*$ regions of [0.45, 0.55), [0.55, 0.65), [0.65, 0.75), and [0.75, 1] are shown in Fig. 1 for the $\sqrt{s} = 10.52$ GeV data sample. The Ξ_c^0 signals are extracted from maximum-likelihood fits to these invariant mass spectra. For Ξ_c^0 semileptonic decays, there are four kinds of background sources: (1) Ξ^- is reconstructed correctly, but ℓ^+ is identified incorrectly; (2) Ξ^- is reconstructed incorrectly, but ℓ^+ is identified correctly; (3) both Ξ^- and ℓ^+ are reconstructed/identified incorrectly; (4) both Ξ^- and ℓ^+ are reconstructed/identified correctly, but they are not from the same Ξ_c^0 decay. The sum of the backgrounds (2) and (3) can be described by the normalized Ξ^- mass sidebands. Invariant mass spectra of wrong-sign $\Xi^- \ell^-$ candidates can describe the backgrounds (1), (3), and (4), and the normalized Ξ^- mass sidebands from $\Xi^- \ell^-$ events can represent the background (3). The possible background from $\Omega_c^0 \rightarrow \Xi^- \ell^+ \nu_\ell$ decay is negligible since it is a $c \rightarrow d$ process and should be suppressed strongly. Considering $SU(3)$ symmetry and the dominance of $\Lambda_c^+ \rightarrow \Lambda e^+ \nu_e$ in inclusive Λ_c^+ semileptonic decay [62], we conservatively take the ratio $\mathcal{B}(\Xi_c^+ \rightarrow \Xi^- \pi^+ \ell^+ \nu_\ell)/\mathcal{B}(\Xi_c^+ \rightarrow \Xi^0 \ell^+ \nu_\ell)$ to be 9%. The differences of signal yields between the fits with and without $\Xi_c^+ \rightarrow \Xi^- \pi^+ \ell^+ \nu_\ell$ component are taken as systematic uncertainties.

Thus, when extracting $\Xi_c^0 \rightarrow \Xi^- \ell^+ \nu_\ell$ signal yields by fitting $\Xi^- \ell^+$ mass spectra in each $p_{\Xi^-X}^*/p_{\text{max}}^*$ bin, as shown in Fig. 1, the signal shapes are directly from the MC simulations, the sum of backgrounds (2) and (3) is described by the normalized Ξ^- mass sidebands and the sum of backgrounds (1) and (4) is described by the selected $\Xi^- \ell^-$ events with their normalized Ξ^- mass sidebands subtracted. In fitting the $\Xi^- \mu^+$ mass spectrum, an additional background of simulated $\Xi_c^{0,+} \rightarrow \Xi^- \pi^+ + \text{anything}$ events from generic MC samples is added. In the fit above, the shapes of all fit components are fixed while their yields are floated. In fitting the $\Xi^- \pi^+$ mass spectrum, the Ξ_c^0 signal shape is parameterized with a double-Gaussian function with same mean value, while the background shape is represented with a 1st-order polynomial. Figure 1 shows the fitted results in each $p_{\Xi^-X}^*/p_{\text{max}}^*$ bin labelled at the bottom for (a) $\Xi_c^0 \rightarrow \Xi^- e^+ \nu_e$, (b) $\Xi_c^0 \rightarrow \Xi^- \mu^+ \nu_\mu$, and (c) $\Xi_c^0 \rightarrow \Xi^- \pi^+$. The fitted result in each $p_{\Xi^-X}^*/p_{\text{max}}^*$ bin together with the corresponding detection efficiency are listed in Table I. The background sources and fit methods are validated with generic MC samples.

The Ξ_c^0 semileptonic decay branching fractions are

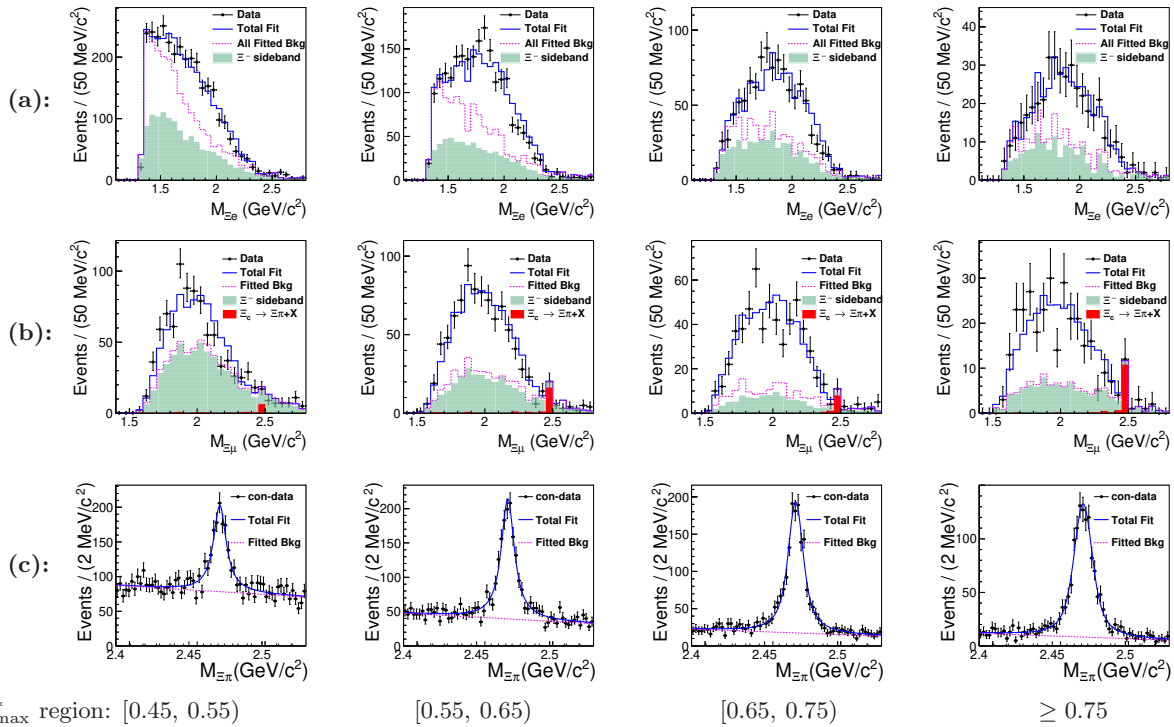


Figure 1: The fits to the $M_{\Xi^- e^+}$, $M_{\Xi^- \mu^+}$, and $M_{\Xi^- \pi^+}$ distributions of the selected (a) $\Xi_c^0 \rightarrow \Xi^- e^+ \nu_e$, (b) $\Xi_c^0 \rightarrow \Xi^- \mu^+ \nu_\mu$, and (c) $\Xi_c^0 \rightarrow \Xi^- \pi^+$ candidates in each $p_{\Xi-X}^*/p_{\max}^*$ bin listed at the bottom. The points with error bars represent the data from the $\sqrt{s} = 10.52$ GeV data sample, the solid blue lines are the best fits, and the violet dashed lines are the fitted total backgrounds.

Table I: List of the fitted signal yields and the corresponding detection efficiencies in each $p_{\Xi-X}^*/p_{\max}^*$ bin ($N_i^{\Xi^- X} / \varepsilon_i^{\Xi^- X}$). The last column gives the ratios of branching fractions $\frac{\mathcal{B}(\Xi_c^0 \rightarrow \Xi^- \ell^+ \nu_\ell)}{\mathcal{B}(\Xi_c^0 \rightarrow \Xi^- \pi^+)}$ in full $p_{\Xi-X}^*/p_{\max}^*$ range. Quoted uncertainties are statistical only.

p_f^*/p_{\max}^*	[0.45, 0.55]	[0.55, 0.65]	[0.65, 0.75]	≥ 0.75	$\frac{\mathcal{B}(\Xi_c^0 \rightarrow \Xi^- \ell^+ \nu_\ell)}{\mathcal{B}(\Xi_c^0 \rightarrow \Xi^- \pi^+)}$
$\Xi_c^0 \rightarrow \Xi^- e^+ \nu_e$	$(8.71 \pm 0.74) \times 10^2 / 15.79\%$	$(9.15 \pm 0.77) \times 10^2 / 18.87\%$	$(5.13 \pm 0.56) \times 10^2 / 21.60\%$	$(2.13 \pm 0.30) \times 10^2 / 22.54\%$	0.954 ± 0.055
$\Xi_c^0 \rightarrow \Xi^- \mu^+ \nu_\mu$	$(3.10 \pm 0.72) \times 10^2 / 6.43\%$	$(5.24 \pm 0.64) \times 10^2 / 10.47\%$	$(4.34 \pm 0.44) \times 10^2 / 14.37\%$	$(2.05 \pm 0.40) \times 10^2 / 17.81\%$	0.952 ± 0.094
$\Xi_c^0 \rightarrow \Xi^- \pi^+$	$(9.41 \pm 0.07) \times 10^2 / 23.36\%$	$(1.29 \pm 0.07) \times 10^3 / 24.71\%$	$(1.51 \pm 0.06) \times 10^3 / 25.91\%$	$(1.22 \pm 0.06) \times 10^3 / 27.13\%$...

calculated using

$$\mathcal{B}(\Xi_c^0 \rightarrow \Xi^- \ell^+ \nu_\ell) \equiv \frac{\varepsilon_{\text{pop}}^{\Xi^- \pi^+} \sum_i \frac{N_i^{\Xi^- \ell^+}}{\varepsilon_i^{\Xi^- \ell^+}}}{\varepsilon_{\text{pop}}^{\Xi^- \ell^+} \sum_i \frac{N_i^{\Xi^- \pi^+}}{\varepsilon_i^{\Xi^- \pi^+}}} \times \mathcal{B}(\Xi_c^0 \rightarrow \Xi^- \pi^+),$$

where $N_i^{\Xi^- X}$ and $\varepsilon_i^{\Xi^- X}$ are the fitted signal yield and detection efficiency, respectively, in each $p_{\Xi-X}^*/p_{\max}^*$ bin; $\varepsilon_{\text{pop}}^{\Xi^- X}$ is the efficiency of the $p_{\Xi-X}^*/p_{\max}^* \geq 0.45$ requirement for each channel and is 0.783, 0.574, and 0.588 for $\Xi_c^0 \rightarrow \Xi^- \pi^+$, $\Xi^- e^+ \nu_e$, and $\Xi^- \mu^+ \nu_\mu$, respectively.

Using the results listed in Table I, we obtain $\mathcal{B}(\Xi_c^0 \rightarrow \Xi^- e^+ \nu_e) = (1.72 \pm 0.10 \pm 0.50)\%$, $\mathcal{B}(\Xi_c^0 \rightarrow \Xi^- \mu^+ \nu_\mu) = (1.71 \pm 0.17 \pm 0.50)\%$, and $\mathcal{B}(\Xi_c^0 \rightarrow \Xi^- e^+ \nu_e) / \mathcal{B}(\Xi_c^0 \rightarrow \Xi^- \mu^+ \nu_\mu) = 1.00 \pm 0.11$. Here, the first and second uncertainties are statistical and from $\mathcal{B}(\Xi_c^0 \rightarrow \Xi^- \pi^+)$ [20], respectively.

We use an additional data sample of 711 fb^{-1} at $\sqrt{s} = 10.58$ GeV to extract the decay parameters of α^+ and α^- , and \mathcal{A}_{CP} for $\Xi_c^0(\bar{\Xi}_c^0) \rightarrow \Xi^- \pi^+(\bar{\Xi}^+ \pi^-)$. In the following, $\Xi_c^0 \rightarrow \Xi^- \pi^+$ and $\bar{\Xi}_c^0 \rightarrow \bar{\Xi}^+ \pi^-$ decays are treated separately to extract α^\pm . To obtain the θ_Ξ distribution, we divided the 2D plane of $p_{\Xi\pi}^*/p_{\max}^*$

versus $\cos\theta_{\Xi}$ into 4×5 bins with the bin edges for $p_{\Xi\pi}^*/p_{\max}^*$ and $\cos\theta_{\Xi}$ set as (0.45, 0.55, 0.65, 0.75, 1.0) and (-1.0, -0.6, -0.2, 0.2, 0.6, 1.0), respectively. The detection efficiency in each 2D bin is calculated individually. The number of $\Xi_c^0(\bar{\Xi}_c^0)$ signal events in each 2D bin is obtained by fitting the corresponding $M_{\Xi\pi}$ distribution with the method used in the branching fraction measurements. The number of signal events in each $\cos\theta_{\Xi}$ bin is the sum of the efficiency-corrected signal yields in corresponding $p_{\Xi\pi}^*/p_{\max}^*$ bins. The fitting method was checked using special MC samples with a range of values of \mathcal{A}_{CP} . The final efficiency-corrected $\cos\theta_{\Xi}$ distributions for (a) $\Xi_c^0 \rightarrow \Xi^-\pi^+$ and (b) $\Xi_c^0 \rightarrow \Xi^+\pi^-$ decays are shown in Fig. 2. Using Eq. (1) with $\alpha_{\Xi^-} = -0.401 \pm 0.010$ and $\alpha_{\Xi^+} = 0.389 \pm 0.009$ [21], the fits yield $\alpha^+ = -0.60 \pm 0.04$ and $\alpha^- = 0.58 \pm 0.04$, resulting in $\mathcal{A}_{CP} = 0.015 \pm 0.052$. Here, the uncertainties are statistical only.

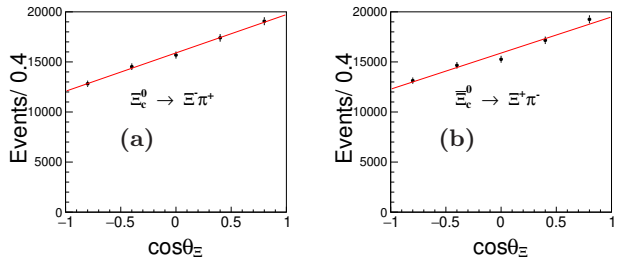


Figure 2: The fits to the efficiency-corrected $\cos\theta_{\Xi}$ distributions of data to extract (a) $\alpha_{\Xi^-\pi^+}$ and (b) $\alpha_{\Xi^+\pi^-}$ for $\Xi_c^0 \rightarrow \Xi^-\pi^+$ and $\Xi_c^0 \rightarrow \Xi^+\pi^-$ decays. The points with error bars represent data from the combined samples at $\sqrt{s} = 10.52$ GeV and 10.58 GeV, and the red solid lines are the best fits.

There are several sources of systematic uncertainties contributing to the branching fraction measurements. Using the $D^{*+} \rightarrow D^0\pi^+$, $D^0 \rightarrow K^-\pi^+$, $\Lambda \rightarrow p\pi$, and $J/\psi \rightarrow \ell\ell$ control samples, the particle identification uncertainties (σ_{PID}) are 0.51% – 0.55% per pion, 0.55% – 0.93% per electron, and 0.44% – 0.84% per muon, depending on the $p_{\Xi-X}^*/p_{\max}^*$ region. The systematic uncertainties associated with tracking efficiency and Ξ^- selection cancel in the branching fraction ratio measurements. We estimate the systematic uncertainties associated with the fitting procedures (σ_{fit}) for $\Xi_c^0 \rightarrow \Xi^-\ell^+\nu_{\ell}$ and $\Xi_c^0 \rightarrow \Xi^-\pi^+$ separately. For $\Xi_c^0 \rightarrow \Xi^-\ell^+\nu_{\ell}$ decays, we change the bin width of $M_{\Xi-\ell^+}$ spectra by ± 5 MeV/ c^2 , change the Ξ^- mass sidebands from two times that of the signal region to three times that of the signal region, or add the background component from $\Xi_c^+ \rightarrow \Xi^-\pi^+\ell^+\nu_{\ell}$, and take the difference of the fitted signal yields as σ_{fit} for each $p_{\Xi-\ell^+}^*/p_{\max}^*$ bin (4.9% – 6.29% for the electron mode and 5.54% – 9.30% for the muon mode). For $\Xi_c^0 \rightarrow \Xi^-\pi^+$, we estimate σ_{fit} by enlarging the mass resolution of signal

shape by 10%, changing the range of the fit and the order of the background polynomial, and take the differences of the fitted signal yields as systematic uncertainties (2.33% – 2.83% depending on the $p_{\Xi^-\pi^+}^*/p_{\max}^*$ region). By using the control sample $\Xi_c^0 \rightarrow \Xi^-\pi^+$, the maximum difference in selection efficiency of the requirement $p_{\Xi-X}^*/p_{\max}^* > 0.45$ between weighted MC simulation based on $p_{\Xi-X}^*/p_{\max}^*$ distribution from data and different signal MC simulations with different fragmentation functions in PYTHIA generator [55] is 3.0%, which is taken as the systematic uncertainty (σ_{epop}). For semileptonic decays, the uncertainties of the form factors in Ref. [56] introduce a 3.1% (3.6% uncertainty in the electron (muon) mode (σ_{FF})). The systematic uncertainties σ_{PID} (σ_{fit}) are added linearly (in quadrature) weighted by $\frac{N_{\Xi^-\pi^+}}{\varepsilon_{\Xi^-\pi^+}}$ and then summed with σ_{epop} and σ_{FF} in quadrature to yield the total systematic uncertainty (σ_B) for each Ξ_c^0 decay mode, which yields 5.8%, 6.3%, and 4.2% for the electron, muon, and pion mode, respectively. The final systematic uncertainty of the branching fraction is the sum of the corresponding two σ_B s in quadrature, which yields 7.2% for $\mathcal{B}(\Xi_c^0 \rightarrow \Xi^-e^+\nu_e)$, and 7.6% for $\mathcal{B}(\Xi_c^0 \rightarrow \Xi^-\mu^+\nu_{\mu})$. The uncertainty of 28.9% on $\mathcal{B}(\Xi_c^0 \rightarrow \Xi^-\pi^+)$ [20] is treated as an independent systematic uncertainty. The total systematic uncertainty for $\mathcal{B}(\Xi_c^0 \rightarrow \Xi^-e^+\nu_e)/\mathcal{B}(\Xi_c^0 \rightarrow \Xi^-\mu^+\nu_{\mu})$ is 8.5%.

The sources of systematic uncertainties in α^{\pm} include fitting procedures ($\sigma_{\text{fit}}^{\alpha^{\pm}}$) and uncertainties on $\alpha_{\Xi^{\pm}}$ values ($\sigma_{\alpha_{\Xi^{\pm}}}^{\alpha^{\pm}}$). $\sigma_{\text{fit}}^{\alpha^{\pm}}$ are estimated with a toy MC method. We use an ensemble of simulated experiments to generate $\cos\theta_{\Xi}$ distributions corresponding to Fig. 2(a) or (b). The number of signal events in each bin is obtained by Gaussian sampling with the mean and width of the Gaussian function set to be the corresponding fitted signal yields and the fitting uncertainty, respectively. After 10,000 simulations, distributions of α^{\pm} , which are found to obey a Gaussian function, are obtained by fitting the slopes of the generated $\cos\theta_{\Xi}$ distributions, and the widths of the Gaussian distributions are regarded as $\sigma_{\text{fit}}^{\alpha^{\pm}}$, which we determine to be $\sigma_{\text{fit}}^{\alpha^+} = 0.2\%$ and $\sigma_{\text{fit}}^{\alpha^-} = 0.2\%$. The uncertainties on $\alpha_{\Xi^{\pm}}$ values are $\sigma_{\alpha_{\Xi^-}}^{\alpha^+} = 2.5\%$ and $\sigma_{\alpha_{\Xi^+}}^{\alpha^-} = 2.3\%$ [21]. The final systematic uncertainties of α^{\pm} are $\sigma_{\alpha^{\pm}} = \sqrt{(\sigma_{\text{fit}}^{\alpha^{\pm}})^2 + (\sigma_{\alpha_{\Xi^{\pm}}}^{\alpha^{\pm}})^2}$. The systematic uncertainty $\Delta_{\mathcal{A}_{CP}}$ is equal to $2\Delta r/(1-r)^2$. Here $r = \alpha^+/\alpha^-$, $\Delta r = |r| \times \sqrt{\sigma_{\alpha^+}^2 + \sigma_{\alpha^-}^2}$. Finally, the systematic uncertainties for α^+ , α^- , and \mathcal{A}_{CP} are estimated to be 0.02, 0.02, and 0.017, respectively.

In summary, based on a data sample of 89.5 fb^{-1} collected with the Belle detector at $\sqrt{s} = 10.52 \text{ GeV}$, we measure the branching fractions of the $\Xi_c^0 \rightarrow \Xi^-\ell^+\nu_{\ell}$ decays. The measured branching fractions are $\mathcal{B}(\Xi_c^0 \rightarrow \Xi^-e^+\nu_e) = (1.72 \pm 0.10 \pm 0.12 \pm 0.50)\%$ and $\mathcal{B}(\Xi_c^0 \rightarrow$

$\Xi^-\mu^+\nu_\mu) = (1.71 \pm 0.17 \pm 0.13 \pm 0.50)\%$. The ratio $\mathcal{B}(\Xi_c^0 \rightarrow \Xi^-e^+\nu_e)/\mathcal{B}(\Xi_c^0 \rightarrow \Xi^-\mu^+\nu_\mu)$ is $1.00 \pm 0.11 \pm 0.09$, which is consistent with the expectation of LFU. Using an additional data sample of 711 fb^{-1} at $\sqrt{s} = 10.58 \text{ GeV}$, the measured Ξ_c^0 decay parameters α^+ and α^- are $-0.60 \pm 0.04 \pm 0.02$ and $0.58 \pm 0.04 \pm 0.02$, respectively. The corresponding average absolute value of α^\pm is $0.59 \pm 0.03 \pm 0.02$ and the CP -asymmetry parameter \mathcal{A}_{CP} of $\Xi_c^0 \rightarrow \Xi^-\pi^+$ decay is measured to be $0.015 \pm 0.052 \pm 0.017$. Here, the first and second uncertainties are statistical and systematic, respectively, while the third uncertainties on branching fractions are due to the uncertainty of $\mathcal{B}(\Xi_c^0 \rightarrow \Xi^-\pi^+)$ [20]. The precision of the measurements of branching fractions of Ξ_c^0 semileptonic decays is greatly improved compared to previous experimental results [18, 19, 48]. We also present the first measurement of the CP asymmetry in Ξ_c^0 decays. The result is consistent with no CP violation.

Y. B. Li acknowledges the support from China Postdoctoral Science Foundation (2020TQ0079). We thank the KEKB group for excellent operation of the accelerator; the KEK cryogenics group for efficient solenoid operations; and the KEK computer group, the NII, and PNNL/EMSL for valuable computing and SINET5 network support. We acknowledge support from MEXT, JSPS and Nagoya's TPRC (Japan); ARC (Australia); FWF (Austria); the National Natural Science Foundation of China under Contracts No. 11575017, No. 11761141009, No. 11975076, No. 12042509; the CAS Center for Excellence in Particle Physics (CCEPP); MSMT (Czechia); CZF, DFG, EXC153, and VS (Germany); DST (India); INFN (Italy); MOE, MSIP, NRF, RSRI, FLRFAS project, GSAC of KISTI and KREONET/GLORIAD (Korea); MNiSW and NCN (Poland); MSHE, Agreement 14.W03.31.0026 (Russia); University of Tabuk (Saudi Arabia); ARRS (Slovenia); IKERBASQUE (Spain); SNSF (Switzerland); MOE and MOST (Taiwan); and DOE and NSF (USA).

[1] J. D. Richman and P. R. Burchat, Rev. Mod. Phys. **67**, 893 (1995).
[2] E. Eichten and B. Hill, Phys. Lett. B **234**, 511 (1990).
[3] M. Neubert, Phys. Rep. **245**, 259 (1994).
[4] M. Kobayashi and T. Maskawa, Prog. Theor. Phys. **49**, 652 (1973).
[5] J. F. Donoghue and S. Pakvasa, Phys. Rev. Lett. **55**, 162 (1985).
[6] M. Ablikim *et al.* (BESIII Collaboration), Phys. Rev. Lett. **115**, 221805 (2015).
[7] M. Ablikim *et al.* (BESIII Collaboration), Phys. Lett. B **767**, 42 (2017).
[8] J. W. Hinson *et al.* (CLEO Collaboration), Phys. Rev. Lett. **94**, 191801 (2005).
[9] J. M. Link *et al.* (FOCUS Collaboration), Phys. Lett. B

634, 165 (2006).
[10] D. Bećirević, S. Fajfer, N. Košnik and O. Sumensari, Phys. Rev. D **94**, 115021 (2016).
[11] A. Crivellin, D. Müller and T. Ota, JHEP **09**, 040 (2017).
[12] D. Buttazzo, A. Greljo, G. Isidori and D. Marzocca, JHEP **11**, 044 (2017).
[13] W. Altmannshofer, S. Gori, S. Profumo and F. S. Queiroz, JHEP **12**, 106 (2016).
[14] A. J. Buras and J. Gérard, JHEP **12**, 009 (2013).
[15] R. Aaij *et al.* (LHCb Collaboration), Phys. Rev. Lett. **122**, 191801 (2019).
[16] R. Aaij *et al.* (LHCb Collaboration), JHEP **08**, 055 (2017).
[17] Y. S. Amhis *et al.* (HFLAV Collaboration), arXiv:1909.12524.
[18] H. Albrecht *et al.* (ARGUS Collaboration), Phys. Lett. B **303**, 368 (1993).
[19] J. P. Alexander *et al.* (CLEO Collaboration), Phys. Rev. Lett. **74**, 3113 (1995).
[20] Y. B. Li *et al.* (Belle Collaboration), Phys. Rev. Lett. **122**, 082001 (2019).
[21] P. A. Zyla *et al.* (Particle Data Group), Prog. Theor. Exp. Phys. **2020**, 083C01 (2020).
[22] Z. X. Zhao, Chin. Phys. C **42**, 093101 (2018).
[23] K. Azizi, Y. Sarac, and H. Sundu, Eur. Phys. J. A **48**, 2 (2012).
[24] C. Q. Geng, Y. K. Hsiao, C. W. Liu, and T. H. Tsai, Phys. Rev. D **97**, 073006 (2018).
[25] C. Q. Geng, C. W. Liu, T. H. Tsai, and S. W. Yeh, Phys. Lett. B **792**, 214 (2019).
[26] R. N. Faustov and V. O. Galkin, Eur. Phys. J. C **79**, 695 (2019).
[27] A. D. Sakharov, Sov. Phys. Usp. **34**, 392 (1991).
[28] A. Riotto, arXiv:hep-ph/9807454.
[29] J. H. Christenson, J. W. Cronin, V. L. Fitch, and R. Turlay, Phys. Rev. Lett. **13**, 138 (1964).
[30] B. Aubert *et al.* (BaBar Collaboration), Phys. Rev. Lett. **87**, 091801 (2001).
[31] K. Abe *et al.* (Belle Collaboration), Phys. Rev. Lett. **87**, 091802 (2001).
[32] B. Aubert *et al.* (BaBar Collaboration), Phys. Rev. D **78**, 034023 (2008).
[33] A. Poluektov *et al.* (Belle Collaboration), Phys. Rev. D **81**, 112002 (2010).
[34] R. Aaij *et al.* (LHCb Collaboration), Phys. Lett. B **712**, 203 (2012) [Erratum: Phys. Lett. B **713**, 351 (2012)].
[35] R. Aaij *et al.* (LHCb Collaboration), Phys. Rev. Lett. **111**, 101801 (2013).
[36] R. Aaij *et al.* (LHCb Collaboration), Phys. Rev. Lett. **110**, 221601 (2013).
[37] R. Aaij *et al.* (LHCb Collaboration), Phys. Rev. Lett. **122**, 211803 (2019).
[38] R. Aaij *et al.* (LHCb Collaboration), Nature Phys. **13**, 391 (2017).
[39] J. G. Körner, G. Krämer, and J. Wilrodt, Z. Phys. C **2**, 117 (1979).
[40] T. Uppal, R. C. Verma, and M. P. Khanna, Phys. Rev. D **49**, 3417 (1994).
[41] G. Kaur and M. P. Khanna, Phys. Rev. D **44**, 182 (1991).
[42] Q. P. Xu and A. N. Kamal, Phys. Rev. D **46**, 270 (1992).
[43] P. Zencykowski, Phys. Rev. D **50**, 402 (1994).
[44] J. G. Körner and G. Krämer, Z. Phys. C **55**, 659 (1992).
[45] H. Y. Cheng and B. Tseng, Phys. Rev. D **46**, 1042 (1992) [Erratum: Phys. Rev. D **55**, 1697 (1997)].

[46] H. Y. Cheng and B. Tseng, Phys. Rev. D **48**, 4188 (1993).

[47] P. Bialas, J.G. Körner, M. Krämer, and Z. Zalewski, Z. Phys. C **57**, 115 (1995).

[48] S. Chan *et al.* (CLEO Collaboration), Phys. Rev. D **63**, 111102 (2001).

[49] K. K. Sharma and R. C. Verma, Eur. Phys. J. C **7**, 217 (1999).

[50] P. Zenczykowski, Phys. Rev. D **50**, 5787 (1994); Phys. Rev. D **50**, 3285 (1994); Phys. Rev. D **50**, 402 (1994).

[51] M. A. Ivanov, J. G. Körner, V. E. Lyubovitskij, and A. G. Tusetsky, Phys. Rev. D **57**, 1 (1998).

[52] Inclusion of charge-conjugate states is implicit unless otherwise stated.

[53] A. Abashian *et al.* (Belle Collaboration), Nucl. Instrum. Methods Phys. Res., Sect. A **479**, 117 (2002); also, see detector section in J. Brodzicka *et al.*, Prog. Theor. Exp. Phys. **2012**, 04D001 (2012).

[54] S. Kurokawa and E. Kikutani, Nucl. Instrum. Methods Phys. Res., Sect. A **499**, 1 (2003), and other papers included in this volume; T. Abe *et al.*, Prog. Theor. Exp. Phys. **2013**, 03A001 (2013) and following articles up to 03A011.

[55] T. Sjöstrand *et al.*, Comput. Phys. Commun. **135**, 238 (2001).

[56] W. Wang, private communication (2021).

[57] D. J. Lange, Nucl. Instrum. Methods Phys. Res., Sect. A **462**, 152 (2001).

[58] R. Brun *et al.*, GEANT, CERN Report No. DD/EE/84-1 (1984).

[59] E. Nakano, Nucl. Instrum. Methods Phys. Res., Sect. A **494**, 402 (2002).

[60] K. Hanagaki *et al.*, Nucl. Instrum. Methods Phys. Res., Sect. A **485**, 490 (2002).

[61] A. Abashian *et al.*, Nucl. Instrum. Methods Phys. Res., Sect. A **491**, 69 (2002).

[62] M. Ablikim *et al.*, (BESIII Collaboration) Phys. Rev. Lett. **121**, 251801 (2018).